

## Sodium-independent carrier-mediated inositol transport in cultured renal epithelial (LLC-PK<sub>1</sub>) cells

Linda M. Russo<sup>a</sup>, Colleen W. Marano<sup>a</sup>, Mary M. Hagee<sup>a</sup>, Kathleen V. Laughlin<sup>a</sup>,  
Anne Guy<sup>b</sup>, Suzanne Varimbi<sup>b</sup>, James M. Mullin<sup>a,\*</sup>

<sup>a</sup> Lankenau Medical Research Center, 100 Lancaster Ave., Wynnewood, PA 19096, USA

<sup>b</sup> Rosemont College, Rosemont, PA, USA

Received 23 December 1994; accepted 3 February 1995

### Abstract

In addition to the concentrative, Na<sup>+</sup>-dependent inositol transport system demonstrated in many cell types, carrier-mediated, Na<sup>+</sup>-independent inositol transport is also shown to exist in LLC-PK<sub>1</sub> renal epithelia. Inhibition of inositol uptake in Na<sup>+</sup>-free saline by 0.1 mM phloretin, and self-inhibition by net concentrations of inositol exceeding 10 mM, demonstrate the carrier-mediation of the Na<sup>+</sup>-independent uptake and distinguish it from flux through anion channels. The Na<sup>+</sup>-dependent uptake exhibits higher affinity for inositol, as seen by the stronger self-inhibition at lower inositol concentrations in Na<sup>+</sup> saline. Kinetic analyses indicate a  $K_m$  of 178  $\mu$ M and a  $V_{max}$  of 2447 pmol/min per  $\mu$ g DNA for the Na<sup>+</sup>-dependent system, whereas the lower affinity, lower capacity Na<sup>+</sup>-independent system manifests a  $K_m$  of 5.2 mM and a  $V_{max}$  of 249 pmol/min per  $\mu$ g DNA. The Na<sup>+</sup>-independent uptake further differs from the Na<sup>+</sup>-dependent transport by the lack of inhibitory effect of 10 mM glucose, and the greater relative inhibition of phloretin compared to that of phlorizin. Both types of uptake appear to localize predominantly to the basal-lateral cell surface. The Na<sup>+</sup>-independent transport is bidirectional, functioning in efflux as well as influx of inositol.

**Keywords:** myo-Inositol; Osmolyte; Facilitated diffusion; Kidney; Phlorizin; Phloretin; Glucose; (Proximal tubule); (LLC-PK<sub>1</sub> cell)

### 1. Introduction

The concentrative, Na<sup>+</sup>-dependent transport of inositol has been described in a wide variety of cell types [1–4]. Since the Na<sup>+</sup> electrochemical gradient is directed into the cell in normal physiological situations, this cotransport system should function only in the concentrative uptake of inositol. Na<sup>+</sup>-independent facilitated diffusional transport can function in both efflux and influx, and unlike simple diffusion through the membrane itself, would be subject to regulation by the cell. Since inositol metabolites are integral signal transduction intermediates [5] and inositol can function in osmoregulation [3], we postulated that a facilitated diffusional inositol transport system would exist. Possible functions for such a transport system would be

regulation of intracellular inositol concentration and/or renal inositol reabsorption. This transport activity, via a unique facilitated diffusional transport system, has been reported in yeast [6] and non-mammalian intestine [7]. We would speculate that many studies exclude a Na<sup>+</sup>-independent inositol transporter because uptake vs. concentration curves for this substrate are normally not performed beyond 5 mM extracellular inositol concentrations. At this concentration, saturability would not be in evidence, and the wrong conclusion could be formed.

The LLC-PK<sub>1</sub> pig kidney epithelial cell line has become a widely studied model for renal proximal tubular and general epithelial transport activity such as glucose uptake [8], phosphate transport [9], Na<sup>+</sup>/H<sup>+</sup> exchange [10], and calcium uptake [11]. At confluence these cells form a polar epithelium which permits not only the study of intracellular inositol uptake and efflux, but, the polar localization of inositol transport systems on either the apical or basal-lateral cell membrane.

\* Corresponding author. Fax: +1 (610) 6458299.

## 2. Materials and methods

### 2.1. Cell line

LLC-PK<sub>1</sub> cells were a gift of Dr. R.N. Hull [12] and were used between passage levels 185 and 200. Cells were routinely passaged weekly by seeding  $1 \cdot 10^5$  cells into a 75 cm<sup>2</sup> culture flask (Falcon) containing 25 ml of  $\alpha$ -minimum essential medium without nucleosides (JRH Biosciences) supplemented with 10% fetal bovine serum (Hyclone) and 2 mM L-glutamine. Cells were suspended for these seedings by rinsing confluent monolayers three times with Ca<sup>2+</sup>/Mg<sup>2+</sup>-free PBS (JRH Biosciences) and incubating at 37°C with 0.25% trypsin/0.02% EDTA (Gibco) until cells detached. Mycoplasma tests based on immunofluorescent assays for Mycoplasma DNA using Hoechst dye [13] were performed every 8–10 weeks and were consistently negative. For routine transport studies, cells were seeded at confluent density into a 100-mm petri dish containing seven 25 mm Nuclepore filters (0.8  $\mu$ m pore) that had been previously collagen-coated (Ethicon) and affixed to the dish. For uptake studies from specifically either the apical or basal-lateral cell surface, cells were seeded at confluent density into 30 mm Falcon 3090 filter cup assemblies. These filter cups do not require collagen coating. Three such filter-cups containing 2 ml of cell suspension were situated in 100-mm petri dishes with 15 ml of culture medium.

### 2.2. Uptake studies

Confluent cell sheets on 25 mm collagen-coated Nuclepore filters were removed from the 100 mm culture dish and rinsed three times in 22°C, 3-(*N*-morpholino)propane sulfonic acid (Mops)-buffered saline [8], then added to a 35 mm petri dish containing 2 ml of this saline with the indicated concentration of *myo*-[2-<sup>3</sup>H(N)]inositol (1–2  $\mu$ Ci/ml) (DuPont NEN; 52.4 Ci/mmol) and 0.1 mM [<sup>14</sup>C]mannitol (1–2  $\mu$ Ci/ml) (Dupont NEN; 55 mCi/mmol). The osmolality of all salines was checked prior to the experiment and determined to be  $300 \pm 6$  mosmol/kg water. Incubations were conducted at 22°C on an orbital shaker, with cell sheets immersed in this saline thereby allowing access to apical and basal-lateral cell surface. Cell sheets were then removed from the incubation saline and passed through five 4°C saline rinses with 0.1 mM phloretin. Cell sheets were then placed in 0.4 M perchloric acid to lyse cells and precipitate DNA. Samples of supernatant were taken for dual label liquid scintillation counting, the D-[<sup>14</sup>C]mannitol counts being used to determine the percentage of [<sup>3</sup>H]inositol counts which were not intracellular. After washing the perchloric acid precipitate with 0.4 M perchloric acid, the precipitated DNA was hydrolyzed in 1 M perchloric acid at 78°C for 45 min. DNA was then assayed spectrophotometrically [14]. Results were calculated as the dpm of [<sup>3</sup>H]inositol

taken into the cells per  $\mu$ g of DNA. For kinetic analyses in Na<sup>+</sup> or Na<sup>+</sup>-free saline (wherein Na<sup>+</sup> is replaced by choline) uptakes of a wide range of inositol concentrations were determined, each at several time points. Uptakes were performed with cell sheets on 25 mm filters as described above. Rates of uptake (pmol/min per  $\mu$ g DNA) were determined from the regression slope of the linear portion of these plots of uptake vs. time. For inhibition analyses, a two-tailed test of significance was applied [15].

When uptake from specifically the apical or the basal-lateral membrane was to be determined, cell sheets were cultured in Falcon 3090 filter-cup assemblies as discussed above. Intactness of the cell sheets was determined by measuring transepithelial resistance of approx. 200 ohms cm<sup>2</sup> with 40  $\mu$ A direct current pulses as described previously [16]. Saline labeled with [<sup>3</sup>H]inositol and [<sup>14</sup>C]mannitol, as above, was added to either the apical or the basal-lateral compartment, with unlabeled saline in the opposite fluid compartment. After incubation, the cell sheet was cut from the filter-cup with a scalpel, and analyses of intracellular inositol and DNA were performed as described above.

### 2.3. Efflux studies

Confluent cell sheets were loaded (90 min) in Na<sup>+</sup> saline with various concentrations of [<sup>3</sup>H]inositol as described above. After this uptake period, one set of cell sheets (control) was rinsed five times in 4°C Na<sup>+</sup>-free saline and analyzed for total dpm per ml cell water, and the percentage of dpm existing as free inositol (see below). The remaining sets of cell sheets were placed in Na<sup>+</sup> or Na<sup>+</sup>-free saline at 22°C with or without inhibitors of efflux, on a rotator for 30 min. Cell sheets were then removed, rinsed five times in 4°C Na<sup>+</sup>-free saline, and analyzed as described above for dpm and DNA.

### 2.4. Chromatographic analyses

A portion of the control cell sheets described above was added to centrifuge tubes containing boiling water, and then boiled for an additional 10 min. After vortexing and centrifuging, the supernatant was evaporated to dryness under vacuum (Savant Speed Vac), redissolved in water, and analyzed by thin-layer chromatography. Cellulose TLC plates (Analtech) and a 4:1 isopropanol/water solvent system were used. Plates were then scanned by the Bioscan 2000 system, using a [<sup>3</sup>H]inositol standard.

### 2.5. Measurement of intracellular total inositol

Cultures of LLC-PK<sub>1</sub> were grown to confluence in 100 mm tissue culture dishes (Falcon). Confluent cultures were rinsed two times with cold PBS and extracted with 0.6 M TCA. The extract was neutralized after five washes with water-saturated ether (1 vol. extract/2 vol. diethyl ether).

Table 1  
Uptake of 25  $\mu\text{M}$  [ $^3\text{H}$ ]inositol in the presence and the absence of  $\text{Na}^+$

	Inositol uptake			
	$\text{Na}^+$ -saline (dpm/ $\mu\text{g}$ DNA/ 15 min)		choline saline (dpm/ $\mu\text{g}$ DNA/ 30 min)	
Control	260 $\pm$ 20	—	32 $\pm$ 6	—
+ 5 mM inositol	5 $\pm$ 1	$P < 0.01$	55 $\pm$ 10	N.S.
+ 0.1 mM phlorizin	87 $\pm$ 5	$P < 0.05$	55 $\pm$ 12	N.S.

Values shown represent the means  $\pm$  S.E. for  $n = 3$ –5 determinations. This experiment was repeated with cells of a later passage, and similar results were obtained. N.S. indicates not significant.

The *myo*-inositol content of the neutralized tissue extract was determined spectrophotometrically as described by MacGregor and Matschinsky [17].

### 3. Results

Investigations of inositol transport in various cell types generally utilize an inositol concentration similar to that normally found in human plasma, i.e., 20  $\mu\text{M}$  to 80  $\mu\text{M}$  [2]. As shown in Table 1, if LLC-PK<sub>1</sub> cells are incubated in a  $\text{Na}^+$ -saline containing 25  $\mu\text{M}$  inositol, the carrier-mediated uptake is readily apparent by the significant inhibition exerted by the glycoside phlorizin, as well as the self-inhibition by inositol itself. This represents a manifestation of the general phenomena of competition and saturability in carrier-mediated transport, phenomena which cannot be present in simple diffusional uptake [18]. There is correspondingly an *apparent* lack of carrier mediation for 25  $\mu\text{M}$  inositol uptake in a  $\text{Na}^+$ -free saline, namely no inhibitory effect of phlorizin nor any self-inhibition by 5 mM inositol (Table 1).

However, since intracellular inositol levels are generally in the millimolar range [19,20], and LLC-PK<sub>1</sub> cells were found to contain a free inositol concentration of  $8.7 \pm 0.6$  mM, we postulated that the more significant comparison

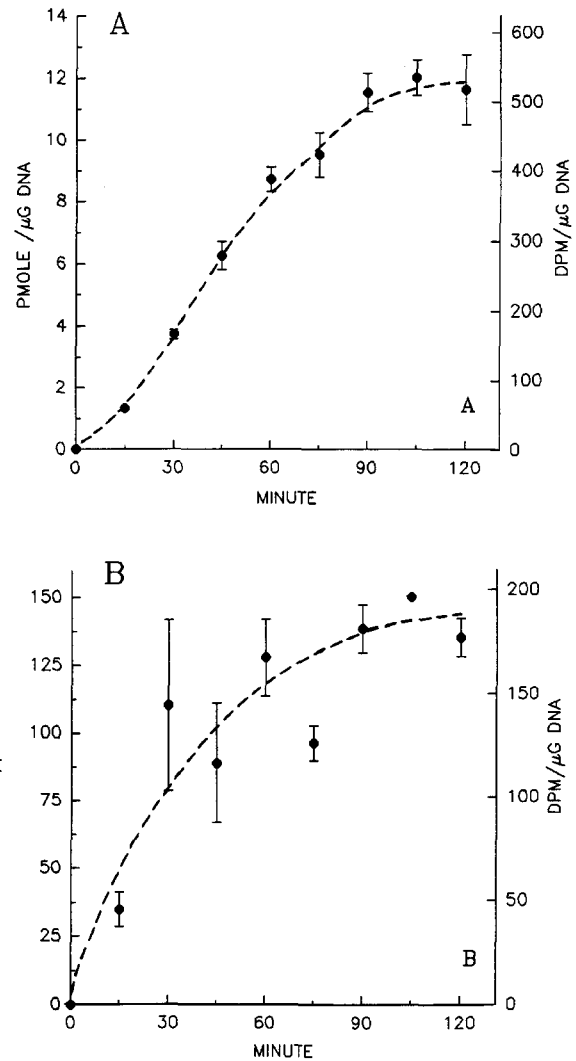


Fig. 1. Time-courses of 25  $\mu\text{M}$  inositol uptake in  $\text{Na}^+$  saline (A) and 5 mM inositol uptake in  $\text{Na}^+$ -free saline (B) by confluent LLC-PK<sub>1</sub> cell sheets. As described in Materials and methods, cell sheets were incubated for up to 120 min at 22° C in either  $\text{Na}^+$  or  $\text{Na}^+$ -free radiolabeled saline, and processed for dpm and DNA. Values shown represent the means  $\pm$  S.E. for  $n = 6$  determinations. These uptakes were repeated with cells of a later passage, and similar time-courses were obtained.

Table 2  
Inhibition of the uptake of 25  $\mu\text{M}$  [ $^3\text{H}$ ]inositol in  $\text{Na}^+$ -saline vs. 5 mM [ $^3\text{H}$ ]inositol in  $\text{Na}^+$ -free saline

	Inositol uptake			
	$\text{Na}^+$ -saline ( $n = 7$ ) (dpm/ $\mu\text{g}$ DNA/15 min)		choline saline ( $n = 6$ ) (dpm/ $\mu\text{g}$ DNA/30 min)	
Control	494 $\pm$ 4	—	56 $\pm$ 4	—
+ 5 mM inositol	5 $\pm$ 5	$P < 0.001$	36 $\pm$ 2	$P < 0.01$
+ 40 mM inositol	N.M.	—	6 $\pm$ 3	$P < 0.001$
+ 10 mM glucose	233 $\pm$ 40	$P < 0.01$	64 $\pm$ 3	N.S.
+ 0.1 mM phlorizin	209 $\pm$ 13	$P < 0.01$	62 $\pm$ 3	N.S.
+ 0.1 mM phloretin	322 $\pm$ 7	$P < 0.01$	41 $\pm$ 5	$P < 0.05$

As described in Materials and methods, confluent LLC-PK<sub>1</sub> cell sheets on collagen-coated filters were incubated in the appropriate radiolabeled saline for 15 min at 22° C with or without the indicated inhibitor. Values shown represent the means  $\pm$  S.E. The experiment was repeated with cells of a later passage and similar results were obtained. N.M. indicates not measured. N.S. indicates not significant.

Table 3

The concentrative accumulation of [ $^3\text{H}$ ]inositol within LLC-PK<sub>1</sub> in the presence of Na<sup>+</sup>

	[ $^3\text{H}$ ]inositol activity in saline (dpm/ml)	Total intracellular $^3\text{H}$ (dpm/ $\mu\text{g}$ DNA)	Intracellular <i>free</i> [ $^3\text{H}$ ]inositol (dpm/ $\mu\text{g}$ DNA)	Intracellular <i>free</i> [ $^3\text{H}$ ]inositol activity (dpm/ml cell water)	$S_i/S_o$
Na <sup>+</sup> saline (25 $\mu\text{M}$ inositol)	$1.24 \cdot 10^6 (\pm 1.6 \cdot 10^4)$	$1119 \pm 52$	$1001 \pm 47$	$1.0 \cdot 10^7 (\pm 0.1 \cdot 10^7)$	$8.23 \pm 0.39$
Choline saline (5 mM inositol)	$7.37 \cdot 10^6 (\pm 3.6 \cdot 10^4)$	$99 \pm 2$	$15 \pm 0.4$	$1.6 \cdot 10^5 (\pm 0.4 \cdot 10^4)$	$0.021 \pm 0.001$

As described in Materials and methods, confluent LLC-PK<sub>1</sub> cell sheets on collagen coated filters were incubated in the appropriate radiolabeled saline supplemented with either 25  $\mu\text{M}$  or 5 mM inositol as indicated for 90 min. Intracellular free [ $^3\text{H}$ ]inositol was determined by thin-layer radiochromatography. The data are presented as the means ( $\pm$  S.E.;  $n = 4$ ). The accumulation of dpm of [ $^3\text{H}$ ]inositol per ml cell water is derived by dividing dpm (free [ $^3\text{H}$ ]inositol)/ $\mu\text{g}$  DNA by  $0.98 \cdot 10^{-4}$  ml cell water/ $\mu\text{g}$  DNA [8].  $S_i/S_o$  is the ratio of the intracellular (free) inositol activity divided by the extracellular (incubation saline) inositol activity. Because the radiochromatography would not account for that amount of [ $^3\text{H}$ ]inositol metabolized by inositol oxygenase with subsequent generation of  $^3\text{H}_2\text{O}$ , no conclusions should be drawn from this data concerning different metabolic fates of inositol following transport via Na<sup>+</sup>-dependent vs. Na<sup>+</sup>-independent pathways.

would be micromolar inositol uptake in Na<sup>+</sup>-saline vs. millimolar inositol uptake in Na<sup>+</sup>-free saline. Although an inositol influx pathway would therefore require affinity only in the  $\mu\text{M}$  range, an inositol efflux system (bidirectional) would require an affinity in the mM range. When we first compare simply the time courses of 25  $\mu\text{M}$  inositol uptake in Na<sup>+</sup>-saline and 5 mM inositol uptake in Na<sup>+</sup>-free saline (Fig. 1), both are near linear over the first 75 min but then both approach steady state by approx. 90 min and clearly plateau by 120 min. Since all [ $^3\text{H}$ ]inositol uptakes are performed as dual-label studies with D-[ $^{14}\text{C}$ ]mannitol also present in the incubation saline (see Materials and methods), the uptakes shown here are at least partially corrected for simple diffusional uptake of inositol. Routinely a percentage of [ $^3\text{H}$ ]inositol dpm are subtracted from the total, based upon the amount of [ $^{14}\text{C}$ ]mannitol dpm in the cell sheet after incubation and rinsings. This percentage is high (occasionally greater than 90%) for Na<sup>+</sup>-free incubations of short duration (less than 15 min) and low (less than 10%) for uptakes in Na<sup>+</sup>-saline of durations of 5 min or longer.

The carrier-mediated nature of the Na<sup>+</sup>-independent uptake of inositol can be seen in the data of Table 2. When 5 mM extracellular [ $^3\text{H}$ ]inositol in Na<sup>+</sup>-free saline is self inhibited by an additional 5 mM inositol, a significant

decrease (36% inhibition) of uptake is observed. 40 mM inositol inhibits the uptake of 5 mM [ $^3\text{H}$ ]inositol (in Na<sup>+</sup>-free saline) to an even greater extent (90% inhibition). This contrasts with the lack of significant inhibition of Na<sup>+</sup>-independent 25  $\mu\text{M}$  [ $^3\text{H}$ ]inositol uptake by 5 mM inositol as shown in Table 1, a frequently applied test purported to show the lack of carrier mediation (in Na<sup>+</sup>-free saline) in many published studies. The key difference between the conditions of Tables 1 and 2 is simply that in Table 2 the *total* concentration of extracellular inositol is raised well above 5 mM, a concentration range in which saturability will be evidenced. Dilution of isotope cannot by itself explain this decreased number of  $^3\text{H}$  dpm in the cells in the presence of added unlabeled inositol in Na<sup>+</sup>-free saline. If entry of [ $^3\text{H}$ ]inositol in Na<sup>+</sup>-free saline was achieved by simple diffusion, the rate of entry of labeled inositol would not be affected by any amount of unlabeled inositol. Only if in the presence of Na<sup>+</sup>-free saline is there competition between labeled and unlabeled inositol for entry into the cell at a finite number of sites (transporters) could a decreased number of intracellular  $^3\text{H}$  dpm actually result.

In Na<sup>+</sup>-saline (Table 2), glucose (52% inhibition) and phlorizin (58% inhibition) both significantly inhibit inositol uptake as shown earlier for the kidney [25]. The

Table 4

Na<sup>+</sup>-independent efflux of inositol by LLC-PK<sub>1</sub> cells

Condition	Total dpm/ $10^6$ cells after efflux period	% of total (initial) dpm	dpm <i>free</i> inositol/ $10^6$ cells after efflux period	% of <i>free</i> inositol (initial) dpm/ $10^6$ cells
Control (no efflux)	$(1446 \pm 97)$	(100) <sup>a</sup>	$(241 \pm 38)$	(100) <sup>b</sup>
Efflux in choline saline	$1259 \pm 55$	87	$54 \pm 9$	22
Efflux in choline saline with 0.1 mM phloretin	$1375 \pm 43$	95	$107 \pm 28$	44

Cell sheets were incubated 90 min at 22° C in Na<sup>+</sup>-saline containing 40 mM [ $^3\text{H}$ ]inositol, passed through five rapid rinses in 22° C choline saline, then placed for 30 min on a rotator in 2 ml of 22° C choline saline with or without 0.1 mM phloretin. Cell sheets were then processed for determination of intracellular radioactivity as described in Materials and methods. Control cell sheets were simply rinsed five times at 4° C after the loading period, and intracellular radioactivity was determined. Values shown represent the means for  $n = 4$  cell sheets  $\pm$  S.E. This experiment was repeated with cells of a later passage and similar results were obtained.

<sup>a</sup> This includes [ $^3\text{H}$ ]inositol metabolites which would not be available for efflux (as determined by TLC of the control condition) and represented 83.5% of total dpm.

<sup>b</sup> This is a reflection of the relative amount of *free* inositol at  $t = 0$  (i.e., available for efflux at the start of the 30 min period). It does not reflect distributions of radiolabel at  $t = 30$  min, since some further metabolism may have occurred even at 22° C.

$\text{Na}^+$ -independent uptake system shows the exact opposite profile, namely an insignificant effect by glucose and a 27% inhibition by phloretin, which contrasts phlorizin's lack of significant inhibition. The inhibitory profiles by phlorizin, phloretin, and glucose on inositol transport in the presence versus the absence of  $\text{Na}^+$  are therefore distinct from each other.

A comparison of intracellular dpm (corrected as de-

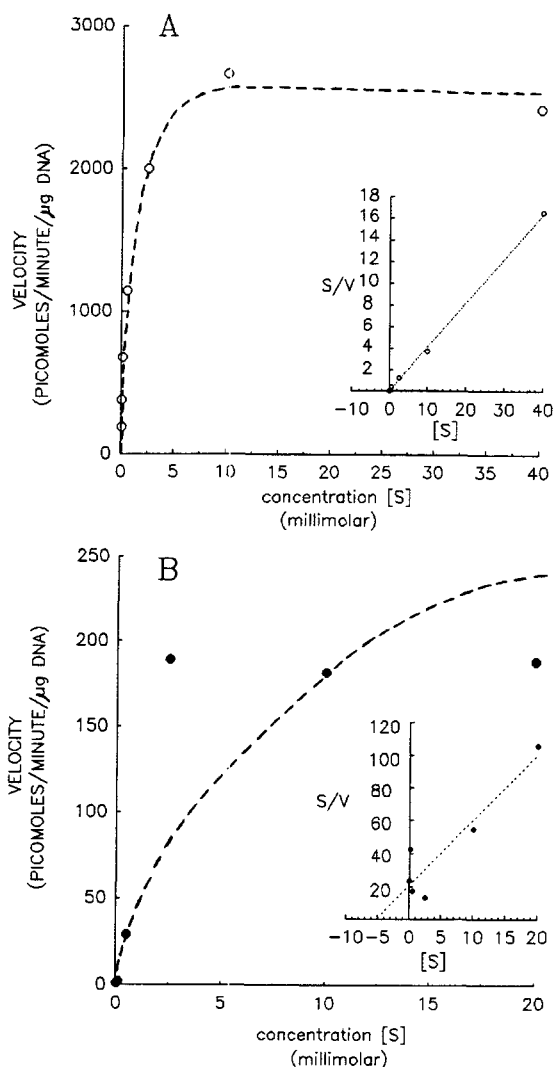


Fig. 2. Velocity vs. substrate concentration for  $\text{Na}^+$ -dependent and  $\text{Na}^+$ -independent inositol uptake by confluent LLC-PK<sub>1</sub> cell sheets. Uptake rates (pmol/min per  $\mu\text{g}$  DNA) are plotted as a function of inositol concentration in  $\text{Na}^+$  (A) or  $\text{Na}^+$ -free saline (B). Uptake rates are determined as described in Materials and methods and then corrected for uptake due to simple diffusion by prior calculation of the  $K_d$  for uptake (due to simple diffusion) at saturating levels of substrate. The curves in both panels are constructed based upon prior determination of  $K_m$  and  $V_{\max}$  by  $S/v_0$  vs.  $S$  plots (see inset), thereby establishing the curves' rate of rise and extent of rise, respectively. The two insets in this figure show plots of the uptake rate data of Fig. 2 according to the form  $S/v = (1/V_{\max})[S] + K_m/V_{\max}$  where the  $K_m$  becomes the absolute value of the  $x$  intercept and the  $V_{\max}$  can be obtained from the reciprocal of the slope.

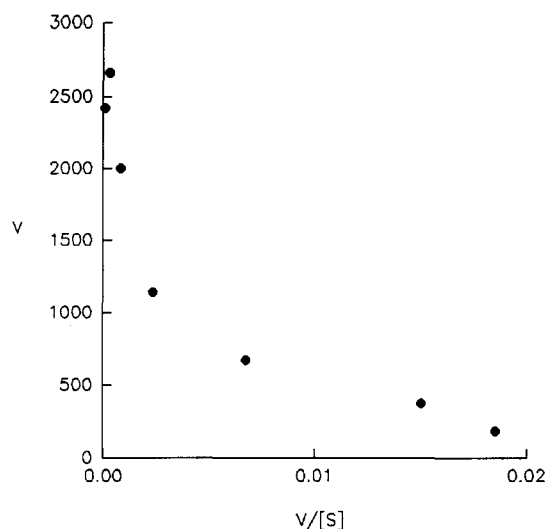


Fig. 3. Eadie-Hofstee plot of the  $\text{Na}^+$ -dependent uptake data.  $V$  vs.  $v/S$  plot of the inositol uptake data in the presence of  $\text{Na}^+$  shown in Fig. 2A.

scribed above for the percentage of intracellular radioactivity which exists as free [ $^3\text{H}$ ]inositol) vs. extracellular radioactivity in the incubation saline illustrates the concentrative vs. non-concentrative nature of inositol transport in  $\text{Na}^+$  vs.  $\text{Na}^+$ -free saline, respectively (Table 3). Specifically, the intracellular radioactivity expressed as dpm/ $\mu\text{g}$  DNA can be multiplied by that percentage of intracellular radioactivity which thin-layer chromatography shows to be free [ $^3\text{H}$ ]inositol, thereby excluding those dpm which are inositol metabolites. This revised dpm (free inositol)/ $\mu\text{g}$  DNA is then divided by the previously described ratio of LLC-PK<sub>1</sub> cell water to DNA ( $0.98 \cdot 10^{-4}$  ml  $\text{H}_2\text{O}_i/\mu\text{g}$  DNA; [8]) to yield an intracellular activity value of dpm/ml  $\text{H}_2\text{O}_i$ . This intracellular activity can then be compared to the extracellular activity of the saline as the ratio  $S_i/S_o$ . As seen in Table 3, this ratio is substantially greater than 1.0 in a  $\text{Na}^+$  saline, and less than 1.0 in a  $\text{Na}^+$ -free saline. This indicates accumulation of radiolabeled free inositol in the presence of  $\text{Na}^+$ , and the inability (after 90 min) to accumulate in the absence of  $\text{Na}^+$ , suggesting concentrative transport operating in  $\text{Na}^+$  saline but not in  $\text{Na}^+$ -free saline. If one assumes steady state conditions (intracellular and extracellular [ $^3\text{H}$ ]inositol specific activities being equal) then the activities reported in Table 3 equate to intracellular inositol concentrations of 0.3 mM for 25  $\mu\text{M}$  extracellular inositol in  $\text{Na}^+$  saline, and 0.2 mM for 5 mM extracellular inositol in  $\text{Na}^+$ -free saline.

To determine kinetic constants for  $\text{Na}^+$ -dependent and  $\text{Na}^+$ -independent inositol uptake, initial velocities of uptake were determined for a wide range of inositol concentrations in  $\text{Na}^+$  saline and  $\text{Na}^+$ -free saline where  $\text{Na}^+$  was replaced by choline. Each reported velocity in these graphs is determined from the slope of the linear regression of amount of uptake vs. time for three time points of inositol uptake at each inositol concentration. Simple diffusional

uptake of inositol (beyond that accounted for by dual label uptakes with [ $^{14}\text{C}$ ]mannitol) was determined by measuring the velocity of uptake at saturating substrate concentrations of inositol (in excess of 10 mM), the slope of this line providing the  $K_d$  for simple diffusion. After correcting the net uptake data for uptake due to simple diffusion, this carrier-mediated uptake was plotted as a function of substrate concentration as shown in Fig. 2A and B. In panel A the uptake in the presence of  $\text{Na}^+$  can be seen to plateau at a velocity of approx. 2500 pmol/min per  $\mu\text{g}$  DNA. In panel B, uptake velocities in the absence of  $\text{Na}^+$  are shown. In this case, the rise to the plateau value is less rapid, and the plateau is significantly lower, only approx. 200 pmol/min per  $\mu\text{g}$  DNA, suggesting a lower capacity system.

The insets to Fig. 2 replot the data in the form of  $S/v$  vs.  $S$ , a plot in which the  $x$  intercept equates to  $-K_m$  and  $V_{\max}$  is approximated by the inverse of the slope of the line, this type of plot being less affected by any contribution of simple diffusion to total uptake [21]. From computer-generated linear plots of these data, the intercepts and slopes yielded a  $K_m$  of 178  $\mu\text{M}$  and a  $V_{\max}$  of 2447 pmol/min per  $\mu\text{g}$  DNA for  $\text{Na}^+$ -dependent uptake, and a relatively low affinity, low capacity,  $\text{Na}^+$ -independent uptake system of 5.2 mM,  $K_m$ , and a  $V_{\max}$  of 249 pmol/min per  $\mu\text{g}$  DNA. The degree and pattern of scatter specifically in the low concentration data of Fig. 2B may be evidence of cooperativity and/or an additional  $\text{Na}^+$ -independent transport system. For the present study, we however assume one ( $\text{Na}^+$ -independent) system for the purposes of kinetic derivations. These kinetic data would also be affected by compartmentalization of cellular inositol, which Berry and coworkers [22] showed to exist in hepatocytes, and which would explain apparent kinetic anomalies of inositol uptake and metabolism.

An Eadie-Hofstee plot ( $v$  vs.  $v/S$ ) of the uptake velocities in the presence of  $\text{Na}^+$  (where both the  $\text{Na}^+$ -dependent and  $\text{Na}^+$ -independent systems would be operative) provides additional evidence for the presence of two dis-

tinct inositol transporters (Fig. 3). Unlike the typical linear plot which would be indicative of a single transport system, our results yielded a curvilinear plot where uptake proceeds by a high capacity, high affinity system at very low substrate concentrations, and then would shift somewhat to a lower capacity, lower affinity system at progressively higher substrate concentrations.

As seen in Table 4, the  $\text{Na}^+$ -independent, phloretin-inhibitable uptake system functions in efflux from the cell as well as uptake into the cell, a result consistent with the general bidirectional nature of  $\text{Na}^+$ -independent facilitated-diffusional transport. After a 90 min uptake of 40 mM [ $^3\text{H}$ ]inositol in  $\text{Na}^+$  saline (22°C), a 30 min efflux in  $\text{Na}^+$ -free saline (22°C) results in the loss of only 13% of total initial intracellular dpm. However, chromatographic analyses of intracellular radioactivity at the end of the uptake period (as in Table 4) showed that only 16% of intracellular dpm existed as free inositol. Therefore, considering only the *free* intracellular radiolabeled inositol, approx. 75% was effluxed. The presence of 0.1 mM phloretin in the efflux saline significantly inhibited the inositol efflux. Instead of losing 75% of intracellular free [ $^3\text{H}$ ]inositol, only 30% was lost with phloretin present in the extracellular saline.

To determine if the  $\text{Na}^+$ -dependent and  $\text{Na}^+$ -independent transport systems are localized on different cell surfaces, the uptake of 25  $\mu\text{M}$  inositol (in  $\text{Na}^+$ -saline) and 5 mM inositol (in  $\text{Na}^+$ -free saline) were compared from the apical vs. basal-lateral fluid compartment (Table 5). In both cases the uptake was markedly greater from the basal-lateral side, suggesting that both the  $\text{Na}^+$ -dependent and  $\text{Na}^+$ -independent inositol transport activity is located, at least predominantly, in the basal-lateral membrane. The amount of uptake which is seen when [ $^3\text{H}$ ]inositol is presented to the apical side (and the fact that it is inhibitable) may be due to inositol in the apical compartment passing between cells (paracellularly through the tight junction) and entering the cell at the basal-lateral membrane, as was shown to be true for glucose analogs [33], or

Table 5

Apical vs. basal-lateral uptake of 25  $\mu\text{M}$  inositol in  $\text{Na}^+$ -saline and 5 mM inositol in  $\text{Na}^+$  free saline

	Inositol uptake (dpm [ $^3\text{H}$ ]inositol/ $\mu\text{g}$ DNA/15 min)			
	apical		basal-lateral	
$\text{Na}^+$ -saline				
25 $\mu\text{M}$ inositol (Control)	157 $\pm$ 11	—	541 $\pm$ 37	—
+ 0.5 mM phlorizin	21.4 $\pm$ 3.1	$P < 0.01$	128 $\pm$ 13	$P < 0.01$
+ 5.0 mM inositol	2.1 $\pm$ 1.0	$P < 0.01$	8.1 $\pm$ 2.7	$P < 0.01$
$\text{Na}^+$ -free saline				
5 mM inositol (Control)	34.2 $\pm$ 1.1	—	226 $\pm$ 9	—
+ 0.5 mM phloretin	2.5 $\pm$ 0.8	$P < 0.01$	100 $\pm$ 12	$P < 0.01$
+ 40 mM inositol	11.9 $\pm$ 1.0	$P < 0.01$	85.1 $\pm$ 4.0	$P < 0.01$

Values shown represent the means  $\pm$  S.E. for  $n = 3$  cell sheets. The experiment was repeated with cells of a later passage, and similar results were obtained.

due to imperfect polar localization of inositol transporters, as we observed for  $\text{Na}^+, \text{K}^+$ -ATPase in these same cells [23].

#### 4. Discussion

Our data indicate that LLC-PK<sub>1</sub> cells possess not only carrier-mediated  $\text{Na}^+$ -dependent but also carrier-mediated  $\text{Na}^+$ -independent inositol transport activity. The bases for this finding on  $\text{Na}^+$ -independent uptake are: (1) self-inhibition of uptake at extracellular inositol concentrations exceeding 5 mM; (2) inhibition of this uptake by phloretin (but not by phlorizin); and (3) the appearance of two transport systems in plots of initial velocities of uptake vs. inositol concentration, one being high affinity, high capacity, the other being low affinity, low capacity. The saturability and phloretin sensitivity of this  $\text{Na}^+$ -independent system in LLC-PK<sub>1</sub> cells fully distinguish it from the inositol flux via anion channels reported for glial cells [24].

There are several observed dissimilarities between  $\text{Na}^+$ -independent and  $\text{Na}^+$ -dependent inositol uptake. First, self-inhibition of  $\text{Na}^+$ -independent uptake occurs in the mM range of concentration rather than the  $\mu\text{M}$  range. As seen in Table 1, attempting to inhibit 25  $\mu\text{M}$  inositol uptake in a  $\text{Na}^+$ -saline with 5 mM inositol is highly effective (greater than 95% inhibition), but in a  $\text{Na}^+$ -free saline it is ineffective. This could erroneously lead to the assumption that  $\text{Na}^+$ -independent uptake in these cells is not carrier mediated. However, if unlike the high affinity,  $\mu\text{M}$  range  $K_m$  of the  $\text{Na}^+$ -dependent system [3,4], the  $\text{Na}^+$ -independent transporter is relatively low affinity, then self-inhibition of this system will not be readily manifested until the net extracellular inositol concentration is brought sufficiently above the  $K_m$  (thereby no longer in the linear portion of a  $V$  vs.  $S$  relation). If the  $K_m$  is of the order of reported *intracellular* inositol levels of 5–10 mM [19,20], then self-inhibition will be manifested only if this concentration is exceeded, as seen in Table 2. Our kinetic data indicate a relatively low affinity (5.2 mM  $K_m$ )  $\text{Na}^+$ -independent inositol transporter, vs. a 178  $\mu\text{M}$   $K_m$  transport system in the presence of  $\text{Na}^+$ . A second dissimilarity is the widely different capacities of the two transport systems, namely  $V_{\max}$  values of 2447 vs. 249 pmol/min per  $\mu\text{g}$  DNA in the presence and absence of  $\text{Na}^+$  respectively.

A third dissimilarity between the  $\text{Na}^+$ -dependent and  $\text{Na}^+$ -independent transport is that  $\text{Na}^+$ -independent uptake appears not to be concentrative. After 90 min at 22°C in a  $\text{Na}^+$ -saline with 25  $\mu\text{M}$  [ $^3\text{H}$ ]inositol, the LLC-PK<sub>1</sub> cells achieve an intracellular free [ $^3\text{H}$ ]inositol activity of  $1.9 \cdot 10^6$  dpm/ml cell water which equates to an intracellular/extracellular concentration gradient of 8.23, expressed as  $S_i/S_o$  (Table 3). However, 90 min in a  $\text{Na}^+$ -free saline with 5 mM [ $^3\text{H}$ ]inositol yields a gradient ( $S_i/S_o$ ) of free [ $^3\text{H}$ ]inositol of only 0.02.

A fourth dissimilarity is the different patterns of inhibi-

tion by glucose, phlorizin and phloretin. Whereas  $\text{Na}^+$ -independent inositol uptake is not significantly inhibited by glucose, and phloretin is a more potent inhibitor than phlorizin,  $\text{Na}^+$ -dependent inositol uptake is inhibited by glucose, and phlorizin is more potent than phloretin. This inhibition by glucose and phlorizin of  $\text{Na}^+$ -dependent inositol uptake has been observed in many preparations [1,25,27]. The description of a  $\text{Na}^+$ -independent, basal-lateral inositol transporter in eel intestine similarly showed inhibition by phloretin but not by phlorizin, but this system was inhibited by glucose and was relatively high affinity [26].

Although another dissimilarity was expected in the polar localization of these two transport systems, both the  $\text{Na}^+$ -dependent and  $\text{Na}^+$ -independent inositol transport activity localized to the basal-lateral cell surface of LLC-PK<sub>1</sub> cells. This is in contrast to the situation for LLC-PK<sub>1</sub> glucose transport, where we previously observed that the  $\text{Na}^+$ -dependent transport system is apical, and the  $\text{Na}^+$ -independent transport system is basal-lateral [28]. It also contrasts with the  $\text{Na}^+$ -dependent and  $\text{Na}^+$ -independent inositol transporters of eel intestine which were also respectively apical and basal-lateral [7,26]. However, the  $\text{Na}^+$ -dependent inositol transporter of MDCK renal epithelia was found to be basal-lateral [29].

As discussed by Baxter et al. [1], the  $\text{Na}^+$ -dependent inositol transporter is present on almost all cell types, differing therein from the  $\text{Na}^+$ -dependent glucose transporter, present chiefly on epithelia engaged in reabsorption. The  $\text{Na}^+$ -dependent inositol transporter's role is apparently concentrative, namely to raise intracellular inositol to mM levels from the  $\mu\text{M}$  levels found in plasma [2], since plasma inositol is the main source of cellular inositol for many cell types. Considering the essential roles played by inositol as a non-ionic osmolyte [3] and by inositol-metabolites in signal transduction [5], we would speculate from our studies that a  $\text{Na}^+$ -independent inositol transporter would be functional in intracellular inositol homeostasis. Being  $\text{Na}^+$ -independent it will function in both efflux and influx as shown in Table 4. Phlorizin-sensitive inositol efflux (which also manifests counter-transport) has recently been shown to occur in hepatocytes [22]. Being a low affinity system, it would essentially have little function until the high affinity,  $\text{Na}^+$ -dependent system elevates cellular inositol levels to a certain range. This range of intracellular inositol concentration will then be a function of *both* the  $\text{Na}^+$ -dependent and  $\text{Na}^+$ -independent inositol carriers. A low capacity, low affinity efflux system operating in tandem with a high capacity, high affinity influx system (as shown by our kinetic data) would be expected for cells to generate the high inositol concentration gradients from *micromolar* levels in serum to *millimolar* levels in cells.

Regulation of the  $\text{Na}^+$ -independent system as a function of extracellular osmolarity will be the subject of future work since the contribution (capacity) of this relatively

low affinity system may increase under certain physiological conditions. Recent findings that extracellular osmolarity will regulate the number of Na<sup>+</sup>-dependent inositol transporters, and thereby the cells' inositol concentrative capacity [24,30–32] attest the overall interest in this area. We submit that the cell's regulatory capacity may extend to Na<sup>+</sup>-independent inositol transporters as well, with the Na<sup>+</sup>-independent system functioning as a 'safety-valve' against excessively high intracellular inositol levels under certain physiological conditions.

## Acknowledgements

We are grateful to Thomas G. O'Brien for his insightful comments during the preparation of this manuscript. We acknowledge the support of NIH Grant CA-48121 to James M. Mullin and a post-doctoral fellowship from Juvenile Diabetes Foundation to Colleen W. Marano. We are also grateful for the assistance in manuscript preparation provided by the Lankenau Medical Research Center editorial staff.

## References

- [1] Baxter, M.A., Bunce, C.M., Lord, J.M., French, P.J., Michell, R.H. and Brown, G. (1991) *Biochim. Biophys. Acta* 1091, 158–164.
- [2] Khatami, M. (1988) *Biochem. Cell Biol.* 66, 942–990.
- [3] Nakanishi, T., Turner, R.J. and Burg, M.B. (1989) *Proc. Natl. Acad. Sci. USA* 86, 6002–6006.
- [4] Olgemoller, B., Schwaabe, S., Schleicher, E.D. and Gerbitz, K.D. (1990) *Biochim. Biophys. Acta* 1052, 47–52.
- [5] Yorek, M.A., Dunlap, J.A. and Stefani, M.R. (1991) *Diabetes* 40, 240–248.
- [6] Nikawa, J.-L., Tsukagoshi, Y. and Yamashita, S. (1991) *J. Biol. Chem.* 266, 11184–11191.
- [7] Reshkin, S.J., Vilella, S., Ahearn, G.A. and Storelli, C. (1989) *Am. J. Physiol.* 256, G509–G516.
- [8] Mullin, J.M., Weibel, J., Diamond, L. and Kleinzeller, A. (1980) *J. Cell. Physiol.* 104, 375–389.
- [9] Scheinman, S.J. (1988) *J. Cell Physiol.* 135, 122–126.
- [10] Haggerty, J.G., Agarwal, N., Reilly, R.F., Adelberg, E.A. and Slayman, C.W. (1988) *Proc. Natl. Acad. Sci. USA* 85, 6797–6801.
- [11] Cheung, J.Y., Constantine, J.M. and Bonventre, J.V. (1986) *Am. J. Physiol.* 251, F690–F701.
- [12] Hull, R.N., Cherry, W.R. and Weaver, G.W. (1976) *In Vitro* 12, 670–677.
- [13] Chen, T.R. (1977) *Exp. Cell Res.* 104, 255–261.
- [14] Burton, K. (1956) *Biochemistry* 62, 315–323.
- [15] Tukey, J.W. (1959) *Technometrics* 1, 31–48.
- [16] Mullin, J.M. and McGinn, M.T. (1987) *FEBS Lett.* 221, 359–364.
- [17] MacGregor, L.C. and Matschinsky, F.M. (1984) *Anal. Biochem.* 141, 382–389.
- [18] Christensen, H.N. (1975) *Biological Transport*, pp. 112–113, W.A. Benjamin, Reading.
- [19] Balaban, R.S. and Burg, M.B. (1987) *Kidney Int.* 31, 562–564.
- [20] Gullans, S.R., Blumenfeld, J.D., Balschi, J.A., Kaleta, M., Brenner, R.M., Heilig, C.W. and Hebert, S.C. (1988) *Am. J. Physiol.* 255, F626–F634.
- [21] Neame, K.D. and Richards, T.G. (1978) *Elementary Kinetics of Membrane Carrier Transport*, pp. 41–55, Blackwell Scientific, Oxford.
- [22] Sigal, H.S., Yandrasitz, J.R. and Berry, G.T. (1993) *Metabolism* 42, 395–401.
- [23] Mullin, J.M., Snock, K.V. and McGinn, M.T. (1991) *Am. J. Physiol.* 260, C1201–C1211.
- [24] Strange, K., Morrison, R., Shrode, L. and Putnam, R. (1993) *Am. J. Physiol.* 265 (Cell Physiol. 34), C244–C256.
- [25] Hammerman, M.R., Sacktor, B. and Daughaday, W.H. (1990) *Am. J. Physiol.* 239, F113–F120.
- [26] Vilella, S., Reshkin, S.J., Storelli, C. and Ahearn, G.A. (1989) *Am. J. Physiol.* 256, G501–G508.
- [27] Whiteside, C.I., Thompson, J.C. and Ohayon, J. (1991) *Am. J. Physiol.* 260, F138–F144.
- [28] Mullin, J.M., McGinn, M.T., Snock, K.V. and Kofeldt, L.M. (1989) *Am. J. Physiol.* 257, F11–F17.
- [29] Yamauchi, A., Kwon, H.M., Uchida, S., Preston, A.S. and Handler, J.S. (1991) *Am. J. Physiol.* 261, F197–F202.
- [30] Kwon, H.M., Yamauchi, A., Uchida, S., Robey, S.B., Garcia-Perez, A., Burg, M.B. and Handler, J.S. (1991) *Am. J. Physiol.* 260, F258–F263.
- [31] Strange, K., Morrison, R., Heilig, C.W., DiPietro, S. and Gullans, S.R. (1991) *Am. J. Physiol.* 260, C784–790.
- [32] Veis, J.H., Molitoris, B.A., Teitelbaum, I., Mansour, J.A. and Berl, T. (1991) *Am. J. Physiol.* 260, F619–F625.
- [33] Mullin, J.M., Fluk, L. and Kleinzeller, A. (1986) *Biochim. Biophys. Acta* 885, 233–239.